

Capillary Rise in Nanopores: Molecular Dynamics Evidence for the Lucas-Washburn Equation

D. I. Dimitrov¹, A. Milchev^{1,2}, and K. Binder¹

⁽¹⁾ *Institut für Physik, Johannes Gutenberg Universität Mainz,
Staudinger Weg 7, 55099 Mainz, Germany*

⁽²⁾ *Institute for Chemical Physics, Bulgarian Academy of Sciences,
1113 Sofia, Bulgaria*

When a capillary is inserted into a liquid, the liquid will rapidly flow into it. This phenomenon, well studied and understood on the macroscale, is investigated by Molecular Dynamics simulations for coarse-grained models of nanotubes. Both a simple Lennard-Jones fluid and a model for a polymer melt are considered. In both cases after a transient period (of a few nanoseconds) the meniscus rises according to a $\sqrt{\text{time}}$ -law. For the polymer melt, however, we find that the capillary flow exhibits a slip length δ , comparable in size with the nanotube radius R . We show that a consistent description of the imbibition process in nanotubes is only possible upon modification of the Lucas-Washburn law which takes explicitly into account the slip length δ . We also demonstrate that the velocity field of the rising fluid close to the interface is not a simple diffusive spreading.

PACS numbers: 47.11.+j, 47.55-t, 47.60.+i, 66.30.-h

Introduction Understanding fluid flow on the nanoscale [1] is crucial for modern developments of nanotechnology like the “lab on a chip” and related nanofluidic devices, as well as for various applications of porous materials, fluid flow through pores in biomembranes, etc. A key process is the ability of fluids to penetrate into fine pores with wettable walls. Filling hollow carbon nanotubes or alumina nanopore arrays with chosen materials opens exciting possibilities to generate nearly one-dimensional nanostructures [2, 3]. In this context, also the filling of silicon dioxide nanochannels [4] and of rolled-up *InAs/GaAs* tubes [5] has found great interest. Related fluid filling phenomena occur when viscous fluid fronts propagate into porous media by spontaneous imbibition [6]. On macroscopic scales, a basic understanding of such capillary rise processes exists for almost a century [7, 8, 9, 10, 11, 12]. However, the applicability of the resulting concepts on the nanoscale has been the subject of a recent controversy [13, 14, 15]. In particular, the conditions under which the Lucas-Washburn equation [7, 8] holds are debated. This equation predicts a \sqrt{t} law for the rise of the fluid meniscus $H(t)$ in the capillary with time t ,

$$H(t) = \left(\frac{\gamma_{LV} R \cos \theta}{2\eta} \right)^{1/2} \sqrt{t}. \quad (1)$$

Here γ_{LV} is the surface tension of the liquid, η its shear viscosity, R the pore radius, and θ the contact angle between the meniscus and the wall. Eq.(1) follows by integration of the differential equation, describing steady state flow, where the capillary force $2\gamma_{LV} \cos(\theta)/R$ is balanced by the viscous drag $4\eta d(H(t)/R)^2/dt$ and one assumes that any possible slip length $\delta \ll R$. Of course,

Eq. (1) cannot be true for $t \rightarrow 0$, but can hold only af-

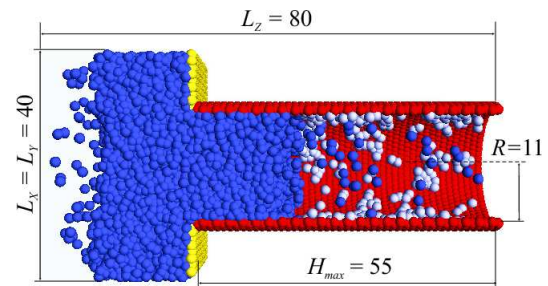


FIG. 1: Snapshot of fluid imbibition in a capillary at time $t = 1300$ MD time steps after the onset of the process. Fluid atoms are shown in blue, those of the precursor film - in light blue. The tube wall is shown in red, and the atoms of the reservoir adhesive wall - in yellow. For further explanations see text.

ter a (nanoscopically small) transient time (Zhmud et al. [11] suggest an initial behavior $H(t) \propto t^2$ when the liquid is accelerated by the capillary forces). However, Mastic et al. [13] find $H(t)$ rising slower than linear with time, even for $t \approx 1ns$, from Molecular Dynamics (MD) simulation of a simple Lennard-Jones (LJ) fluid. They suggest to slightly correct Eq. (1), replacing θ by a dynamic contact angle $\theta(t)$. In contrast, a study of a model for decane molecules in a carbon nanotube [14, 15] yielded a simple linear behavior $H(t) \propto t$ over a wide range of times, leading to the conclusion that filling of nanotubes by fluids does not obey the Lucas-Washburn equation. Experiments so far are inconclusive on this issue, since the existing work [16, 17] deals only with pores that are at least $1 \mu m$ wide. Moreover, in narrow nanotubes an eventual slip at the hydrodynamic boundaries might af-

fect the balance of forces by reducing the viscous drag at the tube wall.

The aim of the present letter is to help clarifying the problem of capillary filling in narrow nanotubes. We present simulations of a generic model, varying both the fluid-wall interaction and the nature of the fluid (simple LJ particles vs. melt of short polymer chains, respectively). Providing independent estimates for all the parameters entering Eq. (1), we are able to perform a decisive test of Eq. (1). Since a fluid flowing into a capillary is a nonequilibrium process, we avoid use of a strictly “microcanonical protocol” of our MD simulations, unlike [14, 15]. Using a dissipative particle dynamics (DPD) thermostat [18], which does not disturb the hydrodynamic interactions due to its Galilean invariance, we maintain strict isothermal conditions, in spite of the heat produced due to the friction of the flowing fluid. In the real system, the walls of the nanofluidic device would achieve the thermostating, of course.

Model description - The snapshot picture, Fig. 1, illustrates our simulation geometry. We consider a cylindrical nanotube of radius $R = 10$, whereby the capillary walls are represented by atoms forming a triangular lattice with lattice constant 1.0 in units of the liquid atom diameter σ . The wall atoms may fluctuate around their equilibrium positions at $R + \sigma$, subject to a finitely extensible non-linear elastic (FENE) potential $U_{FENE} = -15\epsilon_w R_0^2 \ln(1 - r^2/R_0^2)$, $R_0 = 1.5$. Here $\epsilon_w = 1.0k_B T$, k_B denotes the Boltzmann constant, and T is the temperature of the system. In addition, the wall atoms interact by a LJ potential, $U_{LJ}(r) = 4\epsilon_{ww} [(\sigma_{ww}/r)^{12} - (\sigma_{ww}/r)^6]$, where $\epsilon_{ww} = 1.0$ and $\sigma_{ww} = 0.8$. This choice of interactions guarantees no penetration of liquid particles through the wall while in the same time the wall atoms mobility corresponds to the system temperature. In all our studies we use a capillary length $H_{max} = 55$. The right end of the capillary is closed by a hypothetical impenetrable wall which prevents liquid atoms escaping from the tube. At its left end the capillary is attached to a rectangular 40×40 reservoir for the liquid with periodic boundaries perpendicular to the tube axis. Although the liquid particles may move freely between the reservoir and the capillary tube, initially, with the capillary walls being taken distinctly lyophobic, these particles stay in the reservoir as a thick liquid film which sticks to the reservoir lyophilic right wall. The film is in equilibrium with its vapor both in the tube as well as in the left part of the reservoir. At a time $t = 0$, set to be the onset of capillary filling, we switch the lyophobic wall-liquid interactions into lyophilic ones and the fluid enters the tube. Then we perform measurements of the structural and kinetic properties of the imbibition process at equal intervals of time. As a simulation algorithm we use the velocity-Verlet algorithm [19] and DPD thermostat [18, 20] with friction parameter $\xi = 0.5$, Heavyside-type weight functions, and a thermostat cutoff

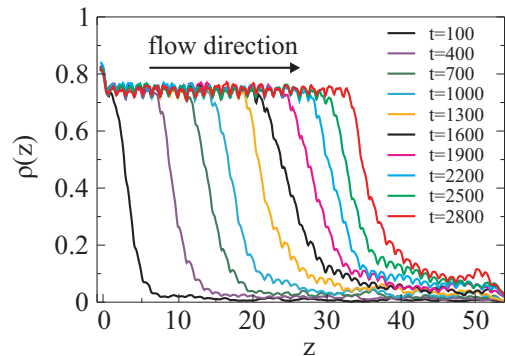


FIG. 2: Profiles of the average fluid density $\rho(z)$ in the capillary at various times for the case $\epsilon_{wl} = 1.4$, $\epsilon = 1.4$. The small oscillations reflect the corrugated structure of the wall of the capillary.

$r_c = 2.5\sigma$. The integration time step $\delta t = 0.01t_0$ where t_0 is our basic time unit, $t_0 = \sqrt{m\sigma^2/48k_B T} = 1/\sqrt{48}$, choosing the particle mass $m \equiv 1$ and $k_B T \equiv 1$.

The capillary filling is studied for two basic cases: (i) a simple fluid interacting via LJ potential with $\epsilon = 1.4$ and $\sigma = 1.0$, and (ii) a non-Newtonian fluid (a polymer melt) consisting of short chains of length $N = 10$. The non-bonded interaction is given by a LJ potential with $\epsilon = 1.4$ and $\sigma = 1.0$ whereas the bonded forces between chain monomers result from a combination of FENE and LJ potentials with $\epsilon = 1.0$ [21]. In both cases the liquid-wall interaction is given by a LJ potential with strength ϵ_{wl} which is varied over a broad range so as to change the wetting characteristics of the system. All interactions are cut off at $r_{cut} = 2.5\sigma$. By varying the interaction strengths and the thermostat parameters, one can change the dynamic properties of the test fluids in a wide range. The total number of liquid particles is 25000 while those forming the tube are 3243.

Simulation results - Typical data for the time evolution of the advancing front of the LJ fluid penetrating into the pore are shown in Fig. 2. Choosing a constant time interval ($\Delta t = 300$) between subsequent profiles in Fig. 2, it is already obvious that the interface position advances into the capillary slower than linear with time! The profiles $\rho(z)$ at late times become distinctly nonzero far ahead of the interface position (near the right wall at $z = 55$ where the capillary ends), due to a fluid monolayer attached to the wall of the capillary: this precursor advances faster than the fluid meniscus in the pore center, but also with a \sqrt{t} law (see below).

Fig. 3a shows that the time evolution of the meniscus height $H(t)$ depends very sensitively on the strength of the wall-fluid interaction (or the contact angle θ , respectively): for $\epsilon_{WS} = 0.6$ and 0.8 only a small number of fluid particles enter the capillary (since $\theta > 90$ for these choices [22]). For $\epsilon_{WS} \geq 1.2$, however, there is only a short transient up to about $t = 250t_0$ (i.e., a time still

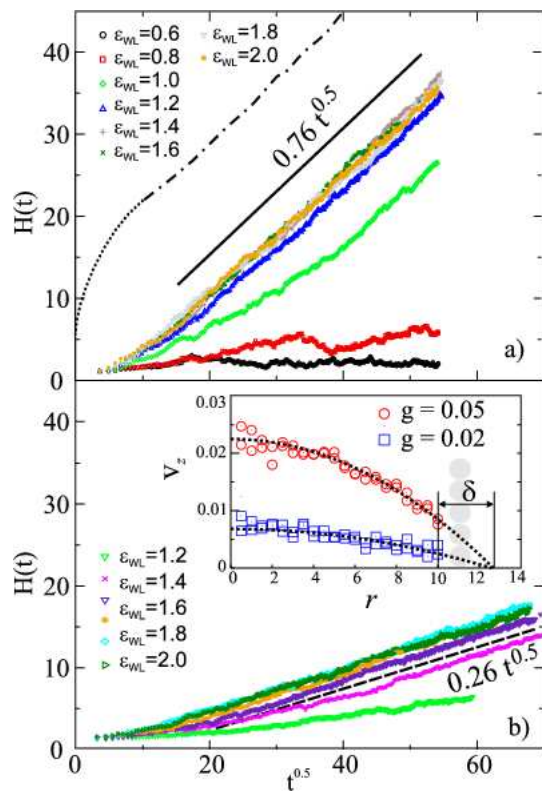


FIG. 3: Position of the liquid meniscus $H(t)$ for a LJ fluid (a), and a melt of decanes (b), for various choices of ϵ_{wl} . The straight lines in (a) - full line, and in (b) - dashed line, indicate the asymptotic law, Eq. (1), in the case of complete wetting. The topmost dash-dotted curve indicates $H(t)$ for the precursor foot (calculated from the total number of particles in the first layer adjacent to the wall of the tube). The initial rise of the precursor (for $t \leq 100t_0$) proceeds much faster, however. The inset in (b) shows the radial velocity variation in a steady flow regime for two strengths of applied external force $g = 0.02$ and $g = 0.05$ (see text) clearly indicating a slip length $\delta \approx 2.7$.

in the nanosecond range), and then a behavior compatible with Eq. 1 is verified. The initial deviation from this law seen in Fig. 3 is not related to the “dynamic contact angle” [13]: this would produce a curvature of opposite sign in Fig. 3. However, in the marginal case $\epsilon_{WL} = 1.0$ a pronounced deviation from Eq. (1) occurs: this curve could be (approximately) fitted to a linear relation, $H(t) \propto t$. It is possible that the results of Supple and Quirke [14, 15] just correspond to such a marginal case. Finally we emphasize that even the height of the precursor foot (topmost curve in Fig. 3a) advances with a $H(t) \propto \sqrt{t}$ law.

To test whether the capillary rise behavior of polymers differs from that of Newtonian fluids, the penetration of a melt of short flexible polymers (above model (ii)) is shown in Fig. 3b. But apart from a general slowing down (attributable to the higher viscosity of the polymer melt), the behavior exhibits the same \sqrt{t} -law.

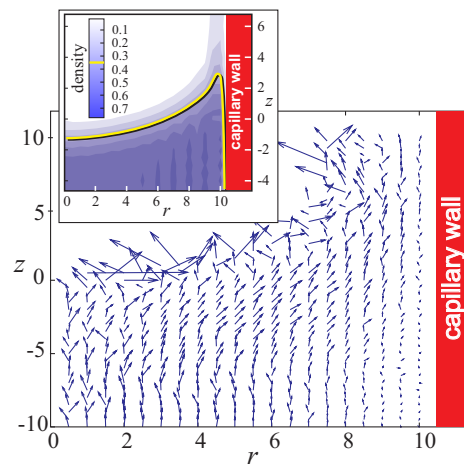


FIG. 4: Velocity field around the moving meniscus for $\epsilon_{wl} = 1.4$. Velocities are averaged within a two-dimensional grid, always fixed at $z = 0$ to the actual *moving* meniscus position and renormalized according to the current meniscus speed. The inset shows the LJ-fluid density profile in the vicinity of the meniscus. The interface position is denoted by a yellow line.

We have also tested whether the results are affected by possible simulation artefacts due to insufficient thermostating conditions. In fact, a slower capillary rise occurs if one uses a “Langevin thermostat” (i.e., an ordinary friction and random noise term acting on all particles), which violates hydrodynamics [23]. A similar result applies if the wall atoms are rigid rather than mobile [22]. But even in these cases the data still follows the \sqrt{t} -law, and also changing details such as the above parameters chosen for the FENE potential of the wall atoms does not matter. From the velocity profiles near the moving meniscus Fig. (4) it is evident that care is needed for the temperature equilibration of such non-equilibrium MD simulations of transient phenomena. The flow is laminar behind the interface, parallel to the walls of the capillary, with the velocity largest in the tube center and going to zero close to the walls. Thus our simple fluid exhibits evidently stick boundary conditions. However, in the interface the velocity field bends over into a direction along the interface, and occasionally particles evaporate into the gas region. This flow pattern shows that the $H(t) \propto \sqrt{t}$ must not be confused with a simple diffusive spreading, of course!

Comparison with the Lucas-Washburn equation - For a test of Eq. 1, it is crucial to also estimate the prefactor, of course, to prove that the \sqrt{t} growth is not just a mere coincidence. For the LJ fluid (at density $\rho_\ell = 0.774$) we find $\eta \approx 6.34 \pm 0.15$, for the polymer melt (at $\rho_\ell = 1.043$) the result is $\eta \approx 205 \pm 25$. We derived compatible values for the viscosity of both fluids also within an equilibrium Molecular Dynamics simulation by using the correlation function of off-diagonal pressure tensor components and the standard Kubo relation [19]. From the

flat gas-liquid interface observed in the left part of our simulation box (Fig. 1) we can estimate the surface tension γ_{lv} from the anisotropy of the pressure tensor [25], $\gamma_{lv} = \int dz \{p_{zz}(z) - [p_{xx}(z) + p_{yy}(z)]/2\}$. This yields $\gamma_{lv} = 0.735 \pm 0.015$ (LJ) and 1.715 ± 0.025 (polymer), respectively.

A consistency check of our results with Eq.(1) is performed for the case of complete wetting, $\cos(\theta) = 1$, which corresponds to $\epsilon_{wl} \geq 1.4$ where the data practically collapse on a single curve. For the simple LJ-fluid with the tube radius $R = 10$ one obtains a slope $H(t)/\sqrt{t} = 0.76 \pm 0.02$ which agrees perfectly with the measured meniscus velocity, cf. Fig. 3a. For the polymer melt, in contrast, Eq.(1) predicts a slope of 0.20 which is considerably less than the observed slopes in Fig. 3b. To clarify this discrepancy we performed MD simulations of steady state Poiseuille flow of identical melt subject to external force g comparable to the capillary driving force. The radial variation of axial velocity indicates a clear slip-flow behavior, cf. inset in Fig. 3b, with a slip length of $\delta \approx 2.7$ which cannot be neglected when compared to the tube radius $R = 10$. The importance of slip-length in processes in the nanoscale range has been emphasized earlier by Barrat and Bocquet [26]. In the present case the existence of a slip length δ can be easily accounted for in the Lucas-Washburn result, Eq.(1), if one notes that, according to the definition of a slip length, the drag force under slip-flow conditions in a tube of radius R and slip length δ is equal to the viscous drag force for a no-slip flow in a tube of effective radius $R + \delta$, that is, to $4\eta d(H(t)/(R + \delta))^2/dt$. In both cases the capillary driving force remains unchanged, $2\gamma \cos(\theta)/R$. Thus one derives a modified Lucas-Washburn relationship:

$$H(t) = \left[\frac{\gamma_{LV}(R + \delta)^2 \cos \theta}{2R\eta} \right]^{1/2} \sqrt{t}. \quad (2)$$

Using Eq.(2), and the material constants given above, we obtain for the slope $H(t)/\sqrt{t} = 0.26 \pm 0.02$ which agrees within errorbars with the observations in Fig. 3b.

Conclusions In summary, we have shown that basic concepts of capillarity such as the Lucas-Washburn equation, Eq. 1, work *almost quantitatively* even at the nanoscale, both for small molecule fluids and complex fluids such as short polymer chains. In case of slip-flow, however, we suggest a simple modification which takes into account the slip length δ . Our new result, Eq. (2), restores the consistency of the Lucas-Washburn law within the framework of the general \sqrt{t} law even in those cases when slip-flow cannot be neglected.

Acknowledgments: One of us (D. D.) received support from the Max Planck Institute of Polymer Research via MPG fellowship, another (A. M.) received partial sup-

port from the Deutsche Forschungsgemeinschaft (DFG) under project no 436BUL113/130. A. M. and D. D. appreciate support by the project "INFLUS", NMP-031980 of the VI-th FW programme of the EC.

-
- [1] A. Meller, J. Phys.: Condensed Matter **15**, R581 (2003)
 - [2] D. Ugarte, T. Stöckli, J. M. Bonard, A. Châtelain, W. A. de Heer, Appl. Phys. A **67**, 101(1998)
 - [3] K. J. Alvine, O. G. Shpyrko, P. S. Pershan, K. Shin, and T. P. Russell, Phys. Rev. Lett. **97**, 175503(2006)
 - [4] S. E. Jarlgaard, M. B. L. Mikkelsen, P. Skafte-Pedersen, H. Bruus, and A. Kristensen, NSTI-Nanotech, www.nsti.org, ISBN 0-9767985-7-3 Vol **2**, 2006
 - [5] C. Deneke and O. G. Schmidt, Appl. Phys. Lett. **85**, 2914(2004)
 - [6] R. Albert and A.-L. Barabási, N. Carle and A. Dougherty, Phys. Rev. Lett. **81**, 2926(1998)
 - [7] R. Lucas, Kolloid. Z. **23**, 15 (1918)
 - [8] E. W. Washburn, Phys. Rev. **17**, 273 (1921)
 - [9] C. H. Bosanguet, Philos. Mag. Ser. 6 **45**, 525 (1923)
 - [10] A. Marmur, in *Modern Approach to Wettability: Theory and Applications* (M. E. Schader and G. Loeb, Eds.) p. 327 (Plenum, New York, 1992)
 - [11] B. V. Zhmud, F. Tiberg, and K. Hallstensson, J. Coll. Interface Sci. **228**, 263 (2000)
 - [12] K. G. Kornev and A. V. Neimark, J. Coll. Interface Sci. **262**, 253 (2003)
 - [13] G. Mastic, F. Gentner, D. Seveno, D. Coulon, J. De Coninck and T. D. Blake, Langmuir **18**, 7971 (2002)
 - [14] S. Supple and N. Quirke, Phys. Rev. Lett. **90**, 214501 (2003)
 - [15] S. Supple and N. Quirke, J. Chem. Phys. **121**, 8571 (2004); *ibid* **122**, 104706(2005)
 - [16] L.-J. Yang, T.-J. Yao, and Y.-C. Tai, J. Micromech. Microeng. **14**, 220 (2004)
 - [17] W. Juang, Q. Lui, and Y. Li, Chem. Eng. Technol. **29**, 716 (2006)
 - [18] P. J. Hoogerbrugge and J. M. V. A. Koelman, Europhys. Lett. **19**, 155 (1992); P. Espanol, Phys. Rev. E **52**, 1734 (1995)
 - [19] M. P. Allen and D. J. Tildesley, *Computer Simulation of Liquids*, Clarendon Press, Oxford, 1987.
 - [20] T. Soddemann, B. Dünweg, and K. Kremer, Phys. Rev. E **68**, 46702 (2003)
 - [21] G. S. Grest and K. Kremer, Phys. Rev. A **33**, 3628 (1986)
 - [22] Full details about our study will be presented elsewhere later.
 - [23] C. Pastorino, T. Kreer, M. Müller, and K. Binder (unpublished)
 - [24] J. A. Baker, C. P. Lowe, H. C. Hoefsloot, and P. D. Iedema, J. Chem. Phys. **122**, 154503 (2005)
 - [25] J. S. Rowlinson and B. Widom, *Molecular Theory of Capillarity* (Clarendon, Oxford, 1982)
 - [26] J.-L. Barrat and L. Bocquet, Phys. Rev. Lett. **82**, 4671 (1999); J.-L. Barrat and L. Bocquet, Faraday Discuss. **112**, 119 (1999)